Perfused Cells, Tissues and Organs by Magnetic Resonance Spectroscopy

Matthew Milkevitch[1], Elizabeth A. Browning[2] & E. James Delikatny[2]

[1] *Philadelphia University, Philadelphia, PA, USA*
[2] *University of Pennsylvania, Philadelphia, PA, USA*

In this article we review methods for the study of perfused cells, tissues, and organs using magnetic resonance spectroscopy (MRS). Biologically relevant nuclei and the different but often complementary information that they make available are presented. Pulse sequence implementation is discussed in the context of tailoring the desired metabolite information and suppressing unwanted resonances. Metabolites observable with MRS are generally limited to those present in relatively high (millimolar) concentrations. The importance of these metabolites and how flux through metabolic pathways can be observed using isotopic enhancement with ^{13}C is reviewed. Cell preparation and immobilization methods employing agarose threads, matrigel and alginate beads; and the use of porous and nonporous microcarriers, hollow fibers and bioreactors for perfused cell culture are discussed. Tissue preparation techniques for the study of perfused organs include the Langendorff heart, perfused liver, and lung preparations. Maintaining careful control of the perfusate composition, pH, oxygenation, and temperature all critically affect cell and organ viability as well as the measured levels of cell metabolites. The requisite apparatus for achieving this is reviewed. Perfusion model systems allow the acquisition of real-time kinetic metabolic information by MRS, providing unique insights into the effects of drugs and inhibitors on metabolite levels. They thus provide a valuable intermediate for translational research from cells to animals to humans and back again.

Keywords: cell perfusion, organ perfusion, NMR, MR spectroscopy, metabolites

How to cite this article:
eMagRes, 2016, Vol 5: 1333 – 1346. DOI 10.1002/9780470034590.emrstm1426

Introduction

One of the great advantages of magnetic resonance (MR) as an analytical biological tool is its ability to translate experimental techniques from cells to animals to humans and back again. A complete MR study allows the comparison of metabolic, physiological, and functional properties of cell and tissue extracts, living cells, organs, and tissues in vitro and in vivo. The development of perfused cell and organ model systems provides an important intermediate for the study of normal biochemistry and physiology as well as the onset and persistence of disease (reviewed in Refs 1–6). In particular, magnetic resonance spectroscopy (MRS) is a powerful tool for the study of metabolism in these controlled environments. MRS provides a quantitative determination of intracellular metabolite concentrations as well as the ability to obtain metabolic information from multiple nuclei, often in a single experiment. Metabolites observable with MRS are generally limited to those present in relatively high (millimolar) concentrations: however, additional metabolites can be observed using isotopic enhancement with carbon-13 (^{13}C) and other nuclei.

The versatility of MRS allows detection of metabolites in perfused cells and organs using a range of nuclei. The available information is complementary to in vivo animal or human spectroscopy data and facilitates translational research. By far, the most common nuclei employed to date have been phosphorus (^{31}P) and ^{13}C to track bioenergetics, pH, and phospholipid, and carbon skeleton metabolism, but many other nuclei have also been employed including the proton (^{1}H), ^{7}Li, ^{19}F, ^{23}Na, ^{35}Cl, ^{39}K and ^{133}Cs. Advances in pulse sequence design have led to the ability to detect intracellular ^{1}H in metabolites in perfused cells against a background of high water concentrations. The advent of hyperpolarized spectroscopy has greatly increased the sensitivity for nuclei such as ^{13}C (see ***Hyperpolarized Carbon-13 MRI and MRS Studies***; ***Integration of ^{13}C Isotopomer Methods and Hyperpolarization Provides a Comprehensive Picture of Metabolism***), which in turn has allowed the dynamic detection of metabolic reactions that were hitherto unattainable.

As in all of MRS, the information available from different isotopes is affected by the relative sensitivity of the nucleus (see Appendix 1), which in turn depends on nuclear spin state, gyromagnetic ratio, natural abundance, and magnetic field strength. These factors impact on hardware and coil design, and on pulse sequence development and use. For perfused cell and organ studies, vertical bore magnets and commercially available coils are most frequently employed. However, the size and shape of ex vivo organs sometimes requires the use of custom coil design or surface coils. All MR pulse sequences are suitable for use in cell and organ preparations, limited only by the spin physics and the imagination of the user. For the most part, pulse sequences chosen for perfused cells and organs are similar to those employed for in vivo MRS, although in the

case of cells, spatial localization is not as crucial owing to the physical dimensions and homogeneity of the sample.

One major difference between perfused cell and organ studies and other forms of MRS is the requirement for a perfusion apparatus to keep tissues in a viable state by controlling nutrient delivery, temperature, pH, and gas delivery. This also allows for the controlled application of drugs, metabolic inhibitors and isotopically labeled substrates. Although the mechanisms used for perfusion remain similar between cells, tissues, and organs, there are a number of specific differences related to sample setup and nutrient requirements between these systems.

Initial Perfused Cell and Organ Studies

The earliest MR studies of cells were performed on packed cell suspensions. The initial measurement of yeast metabolism using ^{13}C-labeled glucose[7] was followed by measurements of intracellular pH in erythrocytes[8] and ortho- and polyphosphates in yeast using ^{31}P MRS.[9] While these seminal studies illustrated the high potential of MRS for determining metabolic factors in biological systems, it was interestingly not cellular MR that benefited initially. Techniques for perfusing organs had been around for over 70 years, and MRS provided an immediate noninvasive solution for tracking metabolism in situ that did not rely on tissue extraction or the analysis of perfusates. A number of studies soon appeared examining nucleoside triphosphate (NTP) levels and pH in perfused heart,[10] liver,[11] and kidney.[12] Early ^{13}C studies focused on the basal metabolism in the liver and metabolic adaptations to drugs and ischemia.[13,14] At this time, the techniques were somewhat limited by the availability of ^{13}C-labeled substrates, but a number of relevant papers appeared tracking glucose and glycogen metabolism, amino acid uptake, and fatty acid metabolism in isolated heart and liver.[14–16]

MR studies of cell suspensions were limited by a lack of oxygen and nutrients in the cell bed that led to rapid depletion of adenosine triphosphate (ATP) and loss of cell viability. To a certain extent, this could be overcome by keeping samples at 4°C to prevent ATP depletion[17] or by studying slow metabolic processes that did not change significantly during the time frame of an experiment, such as mobile lipid metabolites.[18,19] The first perfusion apparatus was built for studies of ^{13}C metabolism in mouse embryonic fibroblasts by Ugurbil in 1981.[20] This was followed by studies of perfused hepatocytes[21,22] to complement studies of perfused liver. Much of the ensuing perfused cell research focused on cancer and cancer metabolism. Part of this was fueled by the availability of a large number of attachment-dependent permanently transformed cell lines. Although the first study employed microcarrier beads for immobilization, a number of additional methods were developed and will be discussed in the section titled 'Cell and Organ Perfusion'.

Isotopic Perfused Cell and Organ Studies

^{13}C MRS

One of the most widespread applications of perfused cells and organs is for tracking the metabolism using ^{13}C labeled substrates. ^{13}C is spin-$^1/_2$, of low natural isotopic abundance (1.108%), and has a gyromagnetic ratio of $\sim^1/_4$ of that of the proton, leading to low sensitivity (1.59×10^{-2} relative to the proton). Natural abundance ^{13}C spectra are relatively featureless (Figure 1); thus ^{13}C-labeled substrates are generally needed for the study of metabolism and metabolic flux. The standard pulse sequence for ^{13}C acquisition is usually a one-dimensional (1-D) pulse-and-acquire experiment with broadband ^{1}H decoupling using WALTZ-16 or a similar multipulse decoupling scheme. Nuclear overhauser enhancement (NOE) is often employed to enhance the signal from the carbon directly bonded to hydrogen.[1,2] For perfused cells, the most commonly used hardware consists of commercially available broadband or dedicated ^{13}C wide-bore probes implemented in a vertical bore scanner with Helmholtz detection coils. Signal-to-noise ratio (SNR) considerations dictate that these experiments are preferentially run at high magnetic field strengths of 9 T or greater, in 10- or 20-mm outer diameter (OD) NMR tubes. Perfused organ studies are most often performed with such a setup, but it is also possible to use horizontal bore magnets with birdcage or similar coils for ^{1}H-MRI. Localization is obtained through the use of surface coils for transmission or detection or both.

An increasing number of ^{13}C-labeled substrates are available commercially or can be custom synthesized. One of the most common is ^{13}C-labeled glucose with [1-$^{13}C_1$] and [U-$^{13}C_6$] being the most readily available substrates. Metabolism of glucose leads to increased labeling in lactate, the end product of glycolysis. Increased labeling is also seen in glutamate that is formed from α-ketoglutarate in the Krebs cycle by α-ketoglutarate transaminase (Figure 1). The low sensitivity of ^{13}C dictates that only metabolites that accumulate at high concentrations are detectable. While uniformly labeled substrates such as [U-$^{13}C_6$] can deliver a higher signal to noise ratio, specific labeling of glucose allows for precise metabolism tracking. For example, metabolism of [1-$^{13}C_1$] glucose will label glutamate at C4 after one passage through the Krebs cycle (Figure 1). By the time the label passes to succinate it is scrambled between the C2 and C3 of this symmetric molecule.[2,23] This results in equal labeling at the C2 and C3 positions of glutamate on second passage through the Krebs cycle.

^{13}C MR studies are reviewed in more detail in ***Integration of ^{13}C Isotopomer Methods and Hyperpolarization Provides a Comprehensive Picture of Metabolism***, but it is worth mentioning that Krebs cycle metabolism can also be accessed through α-ketoglutarate using glutamate or through succinate using labeled propionate.[24,25] ^{13}C-labeled substrates have been used to investigate the role of glutamine as an alternate source of fuel for energy production in cancer and in the perfused heart.[26,27] Of recent interest is the use of labeled glucose to study the role of mutant isocitrate dehydrogenase on aggressive cancer phenotypes.[28] Since muscle tissue relies heavily on β-oxidation for energy, labeled short, medium, and long chain fatty acids have been used to study metabolism under a range of conditions that include normal, ischemic, and diabetic perfused hearts.[29,30]

The focus in liver perfusion has been somewhat different. In addition to probing energy metabolism using the above substrates, investigations of glycogen production and

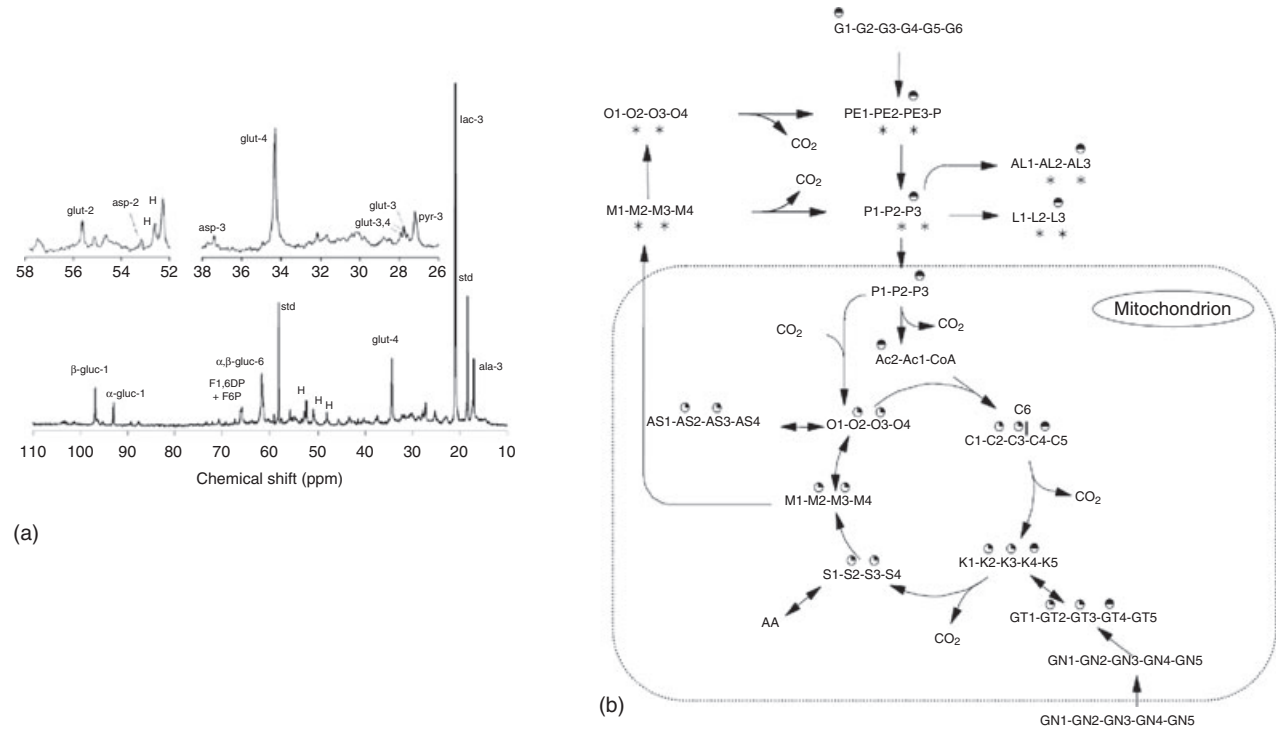

Figure 1. (a) 9.4 T ^{13}C spectrum of EMT6/SF cells during infusion of [1,6-$^{13}C_2$] glucose (bottom). (Reproduced with permission from Ref. 23. © John Wiley & Sons Ltd., 2005.) The spectrum was acquired with a pulse length of 60°, TR = 1200 ms, 4K points, 900 scans, and a spectral width of 25 000 Hz. Bi-level WALTZ-16 decoupling was used to produce NOE enhancement and collapse ^{13}C–^{1}H J couplings. The insert spectra (above) are expansions showing key metabolite resonances. gluc, glucose; lac, lactate; glut, glutamate; asp, aspartate; F1,6DP, fructose 1,6-diphosphate; F6P, fructose-6-phosphate; H, natural abundance ^{13}C in HEPES buffer; Std, natural abundance ^{13}C in an ethanol capillary standard. (b) Metabolic pathway showing the labeling patterns from [1,6-$^{13}C_1$] glucose metabolism entering the Krebs cycle. Glycolysis forms pyruvate labeled at the C_3 position (indicated as P_3 in the figure) (Reproduced with permission from Ref. 2. © Springer, 2004.) [3-$^{13}C_1$] Pyruvate can be further metabolized to [3-$^{13}C_1$] alanine, [3-$^{13}C_1$] lactate, or enter the Krebs cycle in the mitochondria. First round passage (half shaded circles) gives rise to [4-$^{13}C_1$] α-ketoglutarate, which can exit the Krebs cycle by transamination and be observed in ^{13}C -MR spectra as [4-$^{13}C_1$] glutamate. After oxidative decarboxylation the label is scrambled equally between C2 and C4 carbons of succinate (quarter shaded circles in S2 and S3). Second passage through Krebs cycle then gives rise to [2,3-$^{13}C_2$] α-ketoglutarate. Labeled species can also leave the Krebs cycle through malate or aspartate and exit the mitochondrion through the malate–aspartate shuttle. This label can be reincorporated via glycolysis, giving the distinct C2 C3 labeling pattern in pyruvate.

storage, and of gluconeogenesis have been of great interest. Flux through these pathways has been reported using a range of substrates that include glucose, glycerol, pyruvate, and alanine.[31,32] The metabolism of labeled ethanol has also been studied.[33,34] The use of perfused liver allows the examination of the effects of modulators such as insulin and glucagon on these pathways.[31,33,35,36]

Because ^{13}C label tracking is a dynamic process, the flux through various pathways can be measured to estimate reaction rates. There are a number of methods to do this, but most involve solving a series of coupled differential equations.[24,37] Despite the relatively small number of experimental measurements available, detailed information on metabolic flux can still be obtained.

Hyperpolarized ^{13}C MRS. The advent of hyperpolarized technology (see ***Pulse Sequences for Hyperpolarized MRS***; ***Hyperpolarization Methods for MRS***) has led to new interest in ^{13}C-MRS for perfused cell and organs. The ability to prepare labeled substrates with 10^4–10^5 higher levels of ^{13}C nuclear polarization allows for the detection of metabolism with unprecedented SNR. The duration of the non-equilibrium spin polarization is dictated by the spin lattice relaxation time (T_1) of the labeled substrate. As a result, experiments must be performed rapidly, within 5 T_1s, of the polarization transfer. It is thus advantageous to use molecules labeled with ^{13}C on quaternary carbons, such as on a carboxyl group, where the absence of interaction with bound protons results in T_1 relaxation times of tens of seconds. This is in contrast to traditional ^{13}C-labeled MR experiments, where information available from carbon–proton interactions is more desirable. Additional replacement of nearby protons with deuterium can further increase the T_1. These factors require that existing pulse sequences be adapted for optimum detection. The increase in SNR means that localization with ^{13}C is now possible using chemical shift imaging (CSI) sequences. Small flip angles and refocusing are necessary throughout the sequence, since hyperpolarization is lost once all transverse magnetization has dephased.

The majority of hyperpolarized studies have focused on the metabolism of [1-$^{13}C_1$] pyruvate. Pyruvate sits at a central point in intermediary metabolism and can be converted to lactate by glycolysis, to alanine by transamination or decarboxylated with loss of CO_2 by pyruvate dehydrogenase upon entry into

the Krebs cycle. Hyperpolarized pyruvate has been used in perfused cells to compare the glycolytic rate between different cell lines and to monitor the effects of anticancer drugs on glycolysis.[38,39] Pyruvate has been employed to demonstrate enhanced glycolysis in malignant perfused human prostate tissue slices compared to their benign counterparts.[40] Pyruvate metabolism has also been examined in isolated perfused organs including rat heart,[41] mouse liver,[42] and rat lungs.[43] The advent of additional substrates suitable for hyperpolarization,[44] such as [1-^{13}C] α-ketoglutarate to monitor [1-^{13}C] glutamate formation[45] and [1-^{13}C] dihydroascorbate to monitor redox status,[46] will lead to further expansion of this field in the future.

^{31}P MRS

^{31}P has a relatively high SNR from the 100% natural isotopic abundant spin-$^1/_2$ ^{31}P nucleus. It has no background signal, except for the inorganic phosphate (P_i) resonance present in culture medium and a broad baseline signal from the phospholipids bound in cell membranes. ^{31}P MRS of perfused cells and organs is usually performed at high field in a vertical bore scanner with a simple single pulse-and-acquire sequence. The long T_1s and comparatively short spin–spin relaxation times (T_2) and small J-coupling of ^{31}P in phosphate groups allow for relatively rapid sequence repetition periods, TR $\sim$ 1 s, if small pulse flip angles ($\sim$45° or less) are used to optimize SNR efficiency.[1,2] In perfused organs, use of a surface coil is also possible with pulse-and-acquire acquisition; two- or three-dimensional (2-D or 3-D) CSI can be used for enhanced spatial resolution, but the lower sensitivity of the ^{31}P nucleus leads to centimeter-sized voxels that are not useful for organs from rats or mice.

Considerable information is available from ^{31}P spectra. Bioenergetics can be monitored via the 3 NTP resonances that predominantly arise from ATP. In muscle, the additional phosphocreatine (PCr) resonance reports on high-energy phosphate storage. Phospholipid metabolism can be detected through the phosphomonoester (PME) and phosphodiester (PDE) resonances that report on anabolic [phosphocholine (PC) and phosphoethanolamine (PE)] and catabolic [glycerophosphocholine (GPC) and glycerophosphoethanolamine (GPE)] metabolites. pH can also be determined by monitoring the chemical shift of the P_i resonance (Figure 2).

The advent of perfusion techniques made it feasible to monitor cell and tissue bioenergetics in real time. This allowed numerous perfused heart and liver studies of ischemia-reperfusion, metabolic modulators, and of blockers of electron transport and oxidative phosphorylation.[51–55] Not surprisingly, ^{31}P MRS is used routinely to monitor cell or tissue health and proliferation, as the integrated area of the NTP peaks is proportional to viable cell number. In cell studies of cytostatic or cytotoxic drugs, ^{31}P MRS can also be used to monitor ATP depletion due to cell stress and apoptosis.[6,56]

^{31}P MRS is the technique of choice to monitor changes in lipid metabolites.[47,57] The overexpression of choline and ethanolamine kinase in many tumors leads to elevated levels of the phosphomonoesters PC and PE. ^{31}P MRS has been used to measure the kinetics of incorporation of ethanolamine and choline into PC and PE.[58,59] Changes in lipid metabolites can also be used to determine response to anticancer drugs[56,60] by monitoring changes in PC and GPC.[56,61,62] pH measurements using ^{31}P MRS have been useful in understanding changes in acidity resulting from hypoxia and anoxia in perfused

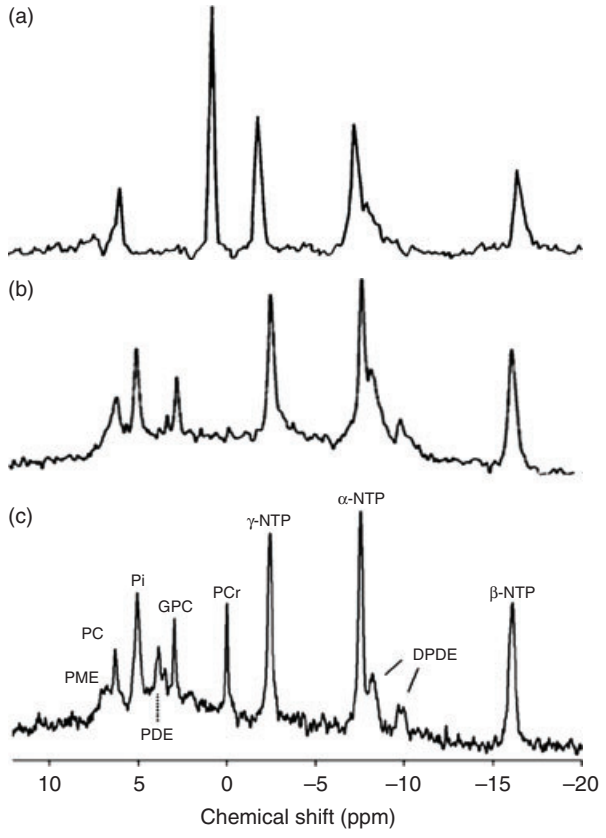

Figure 2. Representative ^{31}P NMR spectra of (a) perfused heart, (b) perfused liver, and (c) perfused EMT6/SF cells are very similar but demonstrate metabolic differences between these systems. All spectra contain the three peaks arising from nucleoside di- and triphosphates (γ-, α-, and β-NTP) and the resonance from inorganic phosphate, P_i. Normal heart contains a strong resonance from PCr. This resonance is absent from the liver, and appears variably in perfused cells depending on their origin. PME (including PC) and PDE (including GPC) are usually observed in perfused cells, but PME levels are dependent upon choline and ethanolamine levels in culture medium.[47,48] The PME and PDE resonances also appear in the liver and are generally small in normal perfused hearts. Deviations from these basic patterns accompany changes in perfusion conditions or the introduction of drugs or antagonists and can be used for detection of altered metabolism. (a) Langendorff preparation of a whole isolated rat heart mounted in a 25 mm diameter NMR tube and perfused with phosphate-free Krebs–Henseleit (KH) buffer at 37°C (acquired at 9.4 T with a 45° flip angle, TR = 2.18 s, number of scans = 104, acquisition time = 4 min). (Reproduced with permission from Ref. 49. © Oxford University Press, 2003.) (b) Isolated rat liver perfused with Krebs–Henseleit buffer for 115 min (acquired at 9.4 T using a ^{31}P/^{13}C double tuned 20 mm probe operating at 9.4 T. 70° flip angle, TR = 0.6 s, number of scans = 240, acquisition time = 2 min). (Reproduced from Ref. 50. © Baillet-Blanco *et al.*; licensee BioMed Central Ltd. 2005.) (c): EMT6/SF spectra were collected at 9.4 T in 5 min in a 20 mm OD NMR tube (60° pulse length, TR = 1 s, 4K points, 1200 scans). (Reproduced with permission from Ref. 23. © John Wiley & Sons Ltd., 2005.) Cells were grown on porous collagen microcarriers mixed 1 : 1 with incompressible polystyrene microspheres. This mixture reduces compression and the resulting pressure gradients across the cell bed

organs.[63,64] This technique has also been used in perfused tumor cell studies to decipher the effects of acidification on metabolism.[62,65]

Finally, it is worth mentioning that saturation transfer experiments have been used extensively to measure the creatine kinase-catalyzed exchange of the phosphate group between ADP and PCr in the perfused heart and muscle.[66,67] This is an important regulatory mechanism that provides short-term replenishment of ATP (see ***Cardiac MRS Studies in Rodents and Other Animals***; ***Measuring Biochemical Reaction Rates In Vivo with Magnetization Transfer***; ***MRS in the Failing Heart: From Mice to Humans***).

^{1}H MRS

For many applications, ^{1}H is the nucleus of choice owing to its high gyromagnetic ratio, 99.98% natural isotopic abundance, and its ubiquitous presence in biological systems. This results in the highest SNR that can be had without hyperpolarization, and enables MRI to be performed. There is a wealth of metabolic information available from ^{1}H spectra including not only water and lipids, but also lipid metabolites (total choline, tCho), creatine, and amino acids (glutamate plus glutamine, Glx) (Figure 3). Even so, the inherently low sensitivity of MR ultimately limits the observable metabolites to those present in relatively high (millimolar) concentrations.

One advantage of ^{1}H MRS is the large number of pulse sequences available. As an example, homonuclear editing has been used to assess lactate concentration in ischemic and anoxic perfused rat hearts.[70,71] Single voxel sequences have been employed for localization including the application of diffusion-weighted (DW) stimulated-echo acquisition mode (STEAM) to measure metabolite apparent diffusion constants (ADCs) in perfused rat hearts.[72] Recently, chemical exchange saturation transfer (CEST) has brought renewed interest to ^{1}H MRS of perfused organs and has been used for the detection of glycogen storage in mouse livers.[36,73]

Perfused cell studies using ^{1}H were initially limited by the large background signal from perfusate water and from nutrients in the culture medium, which can be as high as 10 mM. An elegant solution was developed using a STEAM localization sequence with matched diffusion gradients during the echo time (TE).[74] Adjustment of the diffusion gradients eliminated signals from flowing perfusate spins, allowing the separation of intracellular and extracellular metabolite resonances. As noted earlier, localization is not necessary for most cell perfusion beds; thus a simpler three-pulse DW stimulated echo sequence can also be employed. This led to a number of studies on intracellular metabolism including monitoring of drug response by changes in tCho and mobile lipids.[56,60] Some examples are shown in Figure 3.

^{19}F MRS

^{19}F is spin 1/2, has a 100% natural isotopic abundance, and a gyromagnetic ratio that is 0.94 of the proton, which leads to a relative sensitivity of 0.83. Two great advantages of ^{19}F are that it is of high sensitivity and does not occur naturally. This means that ^{19}F-labeled compounds must be introduced exogenously, but there is no background signal. In perfused cells, the first application of ^{19}F MRS was by Bental and Deutsch, who synthesized and tested a series of labeled pH indicators.[75] In perfused hearts, a number of studies have been performed using ^{19}F labeled pH and calcium indicators (e.g. BAPTA, a calcium-specific aminopolycarboxylic acid).[76] Many drugs contain fluorine and this technique has been used to examine 5-fluorouracil metabolism in perfused mouse liver.[77]

^{23}Na

^{23}Na is a spin 3/2 quadrupolar nucleus with 100% natural isotopic abundance. Although the relative sensitivity of ^{23}Na is 0.0925 compared to ^{1}H, there is still sufficiently high sodium concentration in many tissues to allow the observation of this nucleus. Sodium tissue concentrations and gradients are of particular interest, especially in perfused heart, although a number of studies have also been published on perfused cells and livers. The small chemical shift difference between intracellular and extracellular sodium, along with the quadrupolar broadened line shape, make this distinction difficult to detect. A number of elegant solutions have been designed to this problem including the use of dysprosium or thulium-based paramagnetic reagents to shift the extracellular sodium signal,[78,79] or using MQ filtering[80–82] to enhance the intracellular sodium signal. Recent studies have employed CSI with shift reagents to observe sodium distribution in the perfused heart.[83]

Cell and Organ Perfusion

Perfused Cells

A perfusion system allows for MR studies of whole cells and organs under conditions that are well defined and precisely controlled. For perfused cell experiments, an important requirement is that cells are immobilized in a state most opportune for normal metabolism, growth, and reproduction. The level of immobilization is dependent on cell type and their respective attachment requirements.

Immobilization Methods

Agarose Threads. Agarose is a polysaccharide derived from seaweed. Powdered agarose dissolves in warm water and forms a gel upon cooling. Immobilization of cells in agarose beads or threads (also referred to as filaments) is a commonly used method for MR cell perfusion studies. Cells are introduced into liquid agarose and mixed to provide even distribution. Extrusion using a small-bore sterile syringe will produce threads of a defined diameter that are suitable for insertion into a ≥10 mm OD NMR tube for perfusion with growth media.

Because a variety of adherent and non-adherent cell types can be immobilized using agarose threads, this method has been widely used for perfused cell MRS.[84,85] It has the major advantage of retaining all cells within the immobilization matrix during the MR experiment. This is especially useful for studies of therapeutic response because all cells, living or dead, are retained within the agarose and their total metabolite pool can be monitored. Additional advantages include low cost,

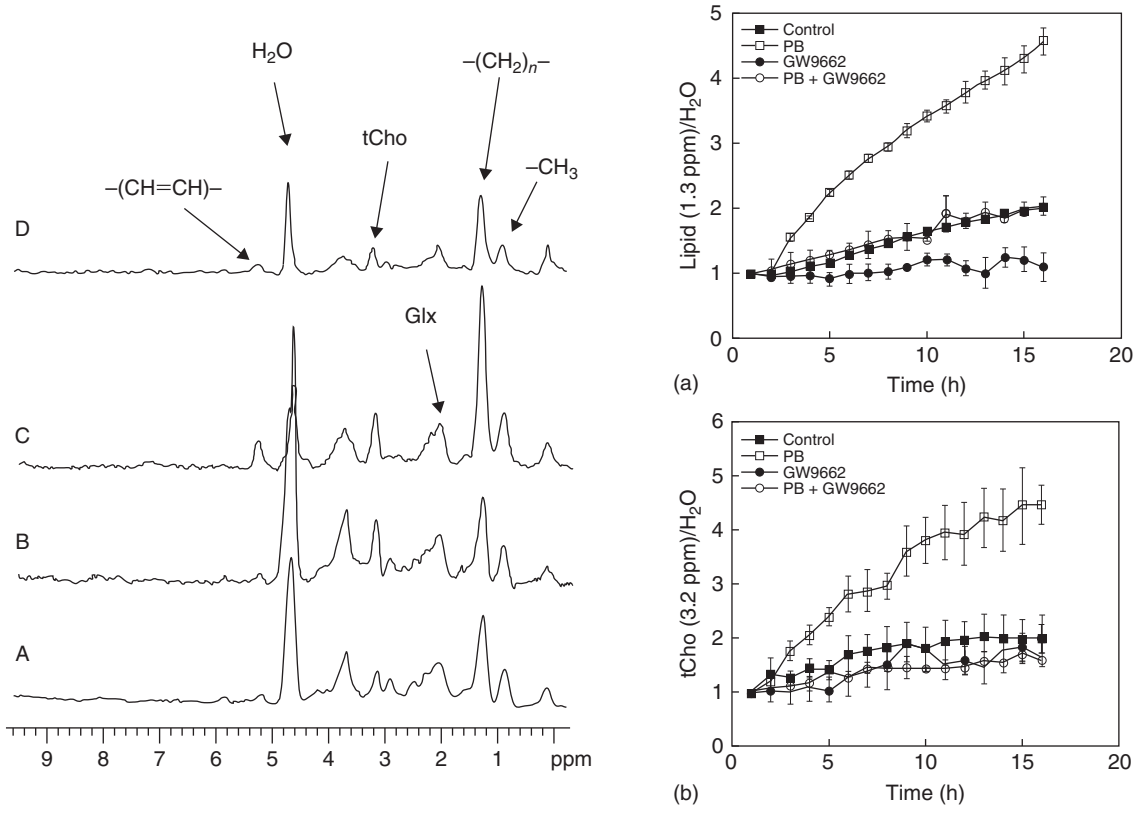

Figure 3. Left: 9.4 T Diffusion-weighted ^{1}H spectra of perfused DU145 prostate cancer cells ($3–4 \times 10^{7}$) grown on Biosilon microcarriers and treated with the differentiating agent phenylbutyrate (PB) in the presence and absence of the PPAR-γ antagonist GW9662 for 16 h. A) control, B) 1 μM GW9662, C) 10 mM PB, D) 1 μM GW9662 and 10 mM PB. Peak assignments are as indicated: the resonance at 0 ppm is a signal originating from the silicon microcarriers. Right: Time-dependent change in ^{1}H-MR resonances relative to the intercellular water resonance. (a) Methylene resonance arising from mobile lipids (1.3 ppm) (b) total choline (tCho) resonance (3.2 ppm). These data show the ability of ^{1}H MRS to track metabolism. The increases in mobile lipid and tCho induced by 10 mM PB (filled spheres) are blocked by addition of 1 μM GW9662 (open spheres) down to control levels (filled boxes). Spectra were acquired at 9.4 T using a 10 mm-multinuclear probe and a perfusion rate of 1.5 ml min^{-1}. A three-pulse diffusion-weighted (DW) pulse sequence was employed to eliminate resonances from flowing water and perfusate and chemical shift-selective (CHESS) water suppression was used to reduce water resonances (TR = 2 s, TE = 21 ms, data size = 2K points, number of scans = 256, acquisition time ~10 min). (Reproduced with permission from Ref. 61. © John Wiley & Sons Ltd., 2010)

facile preparation, and special utility for cells that grow in suspension or that do not have rigorous adherence requirements. A disadvantage is that many cells will not proliferate while immobilized in the threads.

Matrigel. Matrigel is a solubilized basement membrane preparation extracted from Engelbreth-Holm-Swarm (EHS) mouse sarcoma cells. Developed and marketed by Corning Life Sciences, Inc. (Corning, NY, USA), this preparation is rich in proteins such as laminin and collagen IV, and contains several growth factors. It is typically used to produce in vitro cell culture systems that better mimic in vivo environments. Matrigel can also enhance the differentiation and attachment of adherent cells and other cell types.

Matrigel can be utilized to produce threads in a similar manner to agarose. Cells are introduced into the Matrigel in an ice bath, which is then brought to 37 °C to induce cross-linking. The gel is extruded through a syringe or tubing to produce threads.[86,87] Cells are usually seeded at low density and allowed to grow in the threads prior to experimental use.

Because Matrigel mimics the in vivo environment, cells grown using this matrix adopt functions and organizations closer to their in vivo counterparts. In fact, invasive cells can degrade and invade Matrigel. The Bhujwalla group have exploited this to create a metabolic Boyden chamber from Matrigel to measure tumor cell invasion in the magnet.[87] Disadvantages of this immobilization medium include its high cost. The presence of murine growth factors may affect experimental outcomes, and Matrigel can prevent the transport of certain proteins such as ferritin.[88]

Alginate Beads. Sodium alginate is an anionic polysaccharide derived from brown seaweed. This material avidly absorbs water, making it a useful industrial gelling/thickening agent. Cells may be encapsulated by suspending them in an alginate solution, followed by drop-wise addition of the suspension into a solution of $CaCl_2$. The beads formed are collected and transferred to a perfusion apparatus to be perfused with growth media (Figure 4a). The advantages of this method include relatively low cost and applicability

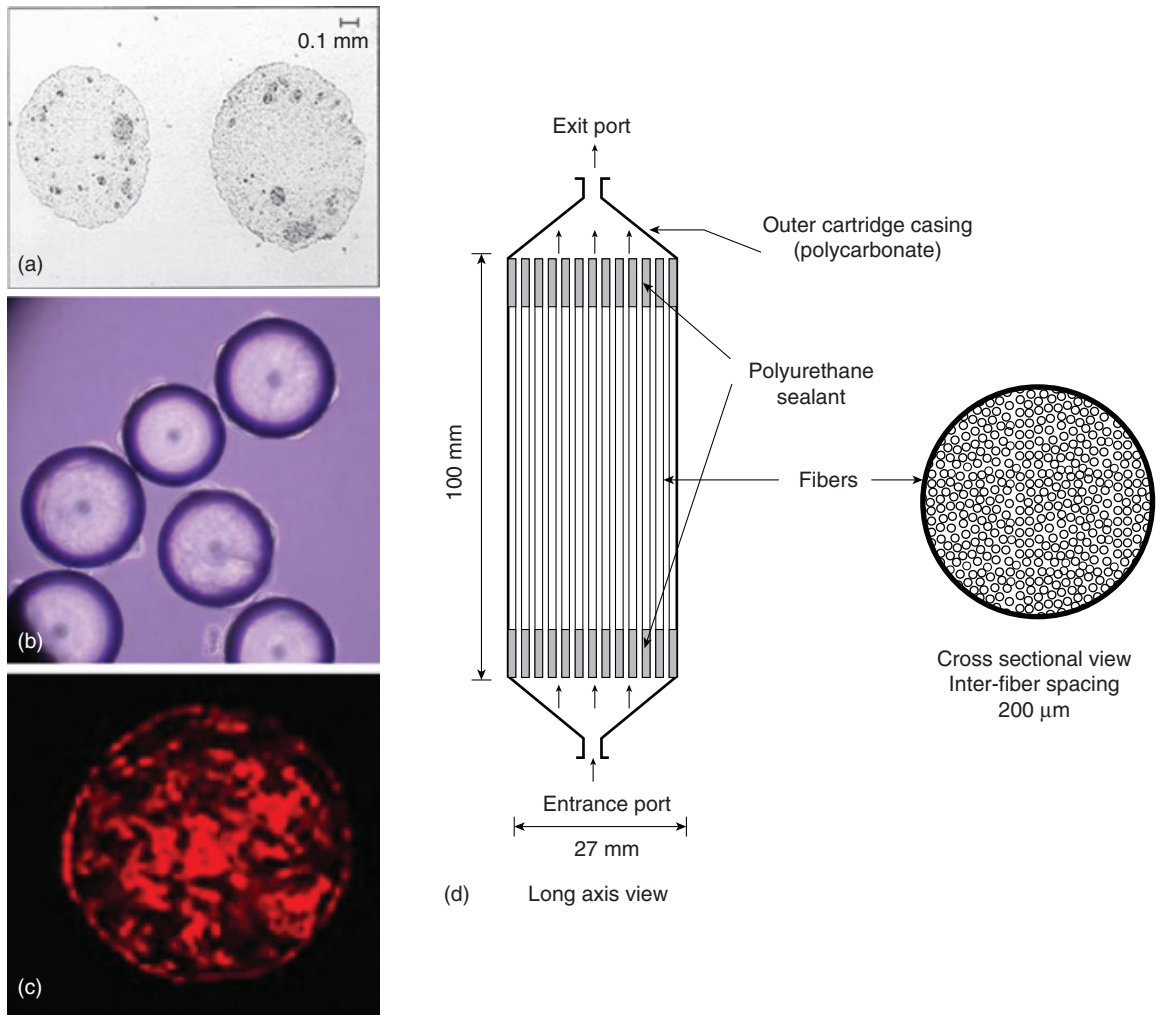

Figure 4. (a) Light micrographs of *β*TC3 mouse insulinoma cells grown on high glucuronic acid alginate beads for 21 days and stained with bromodeoxyuridine to stain DNA. (Reproduced with permission from Ref. 68. © Elsevier, 1999.) (b) Light micrograph of DU145 prostate cancer cells grown on Biosilon microcarriers (160–300 μm diameter). Cells appear as opaque structures adhering to the outside surface of the microcarrier. (Reproduced with permission from Ref. 69. © John Wiley & Sons Ltd., 1993.) (c) Confocal microscopy of SF188 human glioma cells grown inside collagen microcarriers (200 μm average diameter). The microcarriers were stained with propidium iodide to indicate total cellular DNA. (Reproduced with permission from Ref. 23. © John Wiley & Sons, ltd., 2005.) (d) Schematic of a hollow fiber bioreactor including cross-sectional view. Highly porous fibers constitute the internal cell bed at an internal spacing of 200 μm. Cells attach and grow on the outside of the fiber, and receive nutrient media via channels formed from fiber spacing. Media inlet/outlet ports are as indicated.

to a wide variety of cell types. Bead size is an important factor, with nutrient/metabolite diffusion distances and cell density gradients being dependent on the sphere diameter.[5,84,89]

Microcarriers. Microcarriers are another cell immobilization technology currently in use for perfused cell MR studies. One clear advantage microcarriers have is a high surface area-to-volume ratio, making them a viable alternative to monolayer cell culture methods. For perfused cell MR studies, microcarriers are widely used since they allow cells to be conveniently secured in packed beds within large-bore (10 and 20 mm OD) NMR tubes. Microcarriers can be continuously perfused with oxygenated and pH-balanced cell growth medium and then subjected to a variety of studies.

Nonporous Microcarriers. Nonporous microcarriers are solid microcarriers that allow cell attachment and growth on their surface. Coatings that enhance cell attachment can also be applied to the microcarrier. Several types of nonporous microcarriers have been utilized in perfused cell MRS studies (Figure 4b).[20,56,61,90–92] These include dextran microcarriers: Cytodex 1 and 3 (GE Lifesciences, Pittsburgh, PA, USA), polystyrene (untreated, Enhanced Attachment, Synthemax II, collagen coated; Corning Life Sciences, Corning, NY, USA), Biosilon (Nunc; Thermo Fisher Scientific, Waltham, MA, USA, which has been used extensively in MRS but is no longer in production), Solohill (solid core with composition unspecified, solid plastic/coated, animal product free; Pall Corporation, Port Washington, NY USA), and Cultispher (cross linked gelatin; Percell Biolytica, Astorp, Sweden). The various nonporous

microcarriers mentioned above all differ in their size, density, porosity, surface chemistry, and optical properties. Nonporous microcarriers have the disadvantage that the surface coating of cells occupies a small part of the total volume of the sample, which can limit SNR.

Porous Microcarriers. Porous microcarriers contain large, interconnected pores that allow cells to grow both on the surface of the microcarrier and within the cavities defined by the pores (Figure 4c). Given their porous nature, these microcarriers are inherently soft and are therefore compressible.[2] Examples of such microcarriers on the market include Cytopore 1 and 2 (from GE Lifesciences, above), and Pac Microcarriers (ExCel Matrix Biological Devices, Tarnaka, Hyderabad, India). Owing to their compressibility, these microcarriers must be mixed with non-compressible microcarriers in order to be functional for perfused cell MRS studies.[23,93,94]

Hollow Fiber Bioreactors. Hollow fiber bioreactors have been used extensively in the pharmaceutical and biotechnology industry. These bioreactors consist of a closed vessel containing cells and nutrient media in which semipermeable hollow fibers have been inserted (Figure 4d). The hollow fibers function as prototypical 'blood vessels' that facilitate nutrient transport and waste removal from the cells. Hollow fiber bioreactors possess some distinct advantages for perfused MR studies: cells can be grown to high density and sustained for long periods of time (weeks).[69,95,96] However, care must be taken to avoid nutrient gradients resulting from uneven media flow, which can result in heterogeneous cell distributions within the reactor. In order for these reactors to be utilized in perfused cell MRS, either the reactors must be specifically designed with respect to inlet and outlet port placement (i.e., with an axial orientation to the NMR tube) or custom NMR probes must be manufactured. Specific units that fit within 10 and 25 mm NMR probes have been developed.[2,97]

Organ Perfusion

The advantage of using perfused intact organs versus cells is that the structural integrity and functionality of the organ is maintained. This provides the ability to interrogate biochemical signaling and metabolism, intercellular communication between the cell types, and the mechanisms regulating the function of the organ. Motion artifacts caused by respiration and heart contraction in isolated organs can be more easily controlled and regulated to avoid interfering with spectral acquisition and/or image quality. The major drawback is that the organ starts to deteriorate as soon as it is removed from the body despite optimization of the perfusate medium and handling techniques. Accordingly, time is of the essence and reproducibility with the same organ can be challenging. However, study times of several hours are possible and much meaningful information can be obtained using isolated perfused organs that may otherwise not be obtainable in intact animals.

Langendorff Heart. Langendorff published his first perfused heart studies in 1899. In this isolated heart model, the aorta is cannulated and the heart is reverse perfused.[98–100] This results in the aortic valve closing and the coronary arteries filling, which facilitates maintenance of the heart muscle by delivering nutrient-rich media to the heart wall before perfusing the chambers. This allows the heart to stay viable longer than if the chambers are perfused before the feeder vessels. The perfusate can be collected from the right atrium, preventing filling of the heart, but the heart continues to beat as long as the coronary arteries are perfused. This allows for the function of the myocardial wall to be evaluated in the absence or presence of physical and drug-induced loads, therapeutics, substrate levels, and so on. Generally, perfusion with a medium such as Krebs–Ringer Solution is required in order to meet the calcium and glucose demands of the isolated functioning heart.

The Perfused Liver. The isolated perfused rat liver model that was first characterized, developed, and reported by Claude Bernard in 1855 has been widely used for many applications.[101] By cannulating the portal vein, isolated livers can be perfused and maintained viable for ^{13}C and ^{31}P metabolism studies.[31] Much like perfused heart studies, a Krebs bicarbonate buffer at pH 7.4 containing 2% dialyzed bovine serum albumin is generally used in perfused liver studies to maintain ion concentrations and pH, and to satisfy glucose demands.[31] The circulation loop is established by cannulating the portal vein and the vena cava.[102] The perfusate circulates from a reservoir upstream of the portal vein and is collected in a reservoir downstream of the vena cava. The celiac axis and superior mesenteric arteries are generally tied off to establish this flow loop. The liver is then cleared before serum-containing medium or substrate (depending on the study) is recirculated through this loop during longer term metabolic studies.[102]

The Perfused Lung. Isolated perfused lung models have been developed in order to better understand lung function in addition to maximizing the lifespan of isolated lungs for use in organ transplant. In animal models, the trachea is generally cannulated first in order to maintain ventilation. The chest wall is then opened, resulting in degassing of the lungs, and the animal is then rapidly sacrificed via exsanguination. The pulmonary artery and vein are cannulated through the heart, and vascular perfusion can be established. The lung is generally perfused by gravity-driven flow with a Krebs–Ringer or bicarbonate solution supplemented with 10 mM glucose and 5% bovine serum albumin. The perfusate is recirculated with a peristaltic pump.

Perfusates

Central to the technique of perfused MRS is the perfusion medium. Cells, regardless of their origin, need nutrient a supply to grow, divide, and survive. The medium supplies cells with essential building blocks, energy sources, and oxygen, while also regulating pH and serving as a repository for cell waste products. In addition to maintaining cell viability, the medium in a perfused MRS study is also the solvent for the added drugs, antagonists, or labeled substrates whose effects are being investigated.

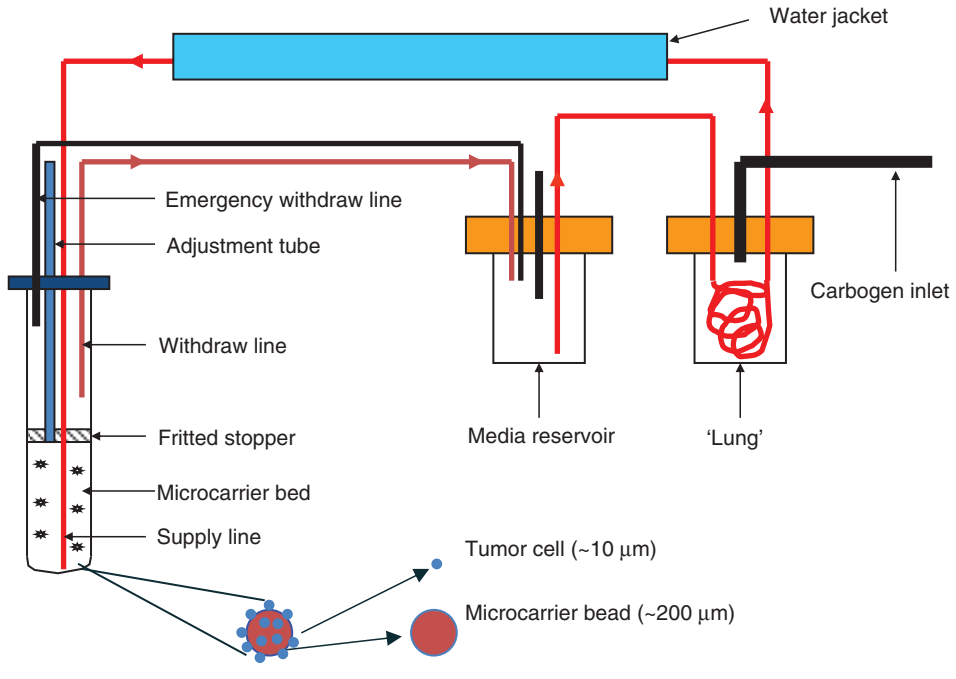

Figure 5. Schematic of the perfusion apparatus used in our laboratory. Cells grown on microcarriers are arranged in a packed bed and constrained under a small-pore polystyrene filter (fritted filter) within a large-bore NMR tube. Oxygenated, pH-controlled medium is pumped from a reservoir through an oxygenation chamber (lung) and then transported to the microcarrier bed in the NMR tube. Introduction and removal of media from the microcarrier bed is accomplished using small-bore Teflon tubing. An emergency media withdraw line is also included to insure no media overflow in the scanner. Media reservoir, 'lung', and media input lines are all thermostatically controlled (37 °C) by either a water bath or a water-jacket, respectively. Carbogen indicates an oxygen/5% CO_2 mixture

Perfusate Composition. The nutritional requirements of perfused cells are met by a culture medium, which generally includes glucose, amino acids, phospholipid precursors (choline, inositol), and vitamins. For perfused organs, a modified Krebs buffer is often used, along with magnesium and calcium in a phosphate carbonate buffer. Glucose or its derivatives (citrate, pyruvate, acetate, and lactate) are supplied as a carbon source and may be experiment specific. In addition to these substances, cells and perfused tissues also require a protein source in order to survive. In isolated cell perfusion models, serum in the form of fetal calf serum is generally used, whereas bovine serum albumin is often used in perfused organ models. The medium helps control the pH and osmolality of the culture, through the inclusion of buffers.

Perfusate pH. pH is commonly regulated in tissue culture through the use of suitable buffers in the growth media, coupled with a properly adjusted incubator atmosphere. Common buffers include phosphate ($pK_a = 7.4$), bicarbonate–CO_2 buffers ($pK_a = 6.4$), and HEPES (4-(2-hydroxyethyl)-1-piperazineethanesulfonic acid) ($pK_a = 7.0$). If a medium containing bicarbonate is used, external CO_2 must be supplied at a level of 5–7% to achieve the proper pH balance. pH monitoring can be facilitated by the inclusion of appropriate indicators.

The Perfusion Apparatus

The primary function of the perfusion apparatus is one of life support. The apparatus supplies and circulates oxygenated perfusion media to the cell bed or organ and extracts it as it exits the cell bed. In addition, the apparatus may warm the perfusate and serve as the solvent reservoir for any drugs or tracers utilized in the study (Figure 5). In order to achieve this function, the perfusion apparatus must include pumps to supply and extract the perfusate from the cell bed, an oxygenation capability ('lung'), media warming capability, media supply/extraction lines, and finally the sample itself. In the following sections, these systems will be discussed individually.

Perfusion System Pumps

Peristaltic Pumps. The pump of choice for a perfusion apparatus is the peristaltic pump. A peristaltic pump is a positive displacement pump consisting of a flexible tube installed within a circular pump casing containing a rotor. The rotor may contain several rollers (or feet), which contact and compress the flexible tube. Turning the rotor produces positive pressure, forcing liquid through the tube and hence throughout the perfusion apparatus.

Peristaltic pumps are typically used to move sterile liquids since the liquid does not come into direct contact with pump components. This is ideal for perfused cell and organs wherein the perfusion media must be kept sterile. In addition, fluids

are pumped at or near ambient pressure, thereby reducing the chances of fluid leaks. Disadvantages of these pumps include tubing wear (requiring occasional replacement), lack of linear flow of fluid at low speeds, and no provision for air bleed within the pump.

Peristaltic Pumps: Usage Considerations. The choice of peristaltic pump for perfused cell experiments is important and several characteristics must be considered including the size of the pump, diameter of tubing accepted by the rotor, available rotational speeds, and level of speed control (fine/coarse). It is often advantageous to run a separate supply pump (inlet to the sample) and an extraction pump (outlet from the sample). This will allow for different rates of supply and removal of media, thereby reducing the chance of perfusate overflow during the experiment. It is important that these pumps are reliable since perfusion experiments can be long (24+ h) and pump failure can prove disastrous to experiments and equipment.

Syringe pumps are also commonly used in perfusion systems because they easily allow a closed system to be maintained, which is ideal for maintaining sterility. They also allow for better control of flow profile, be it unidirectional, laminar, or oscillatory flow. The primary drawback of this type of pump is that the duration of the experiment is limited by the volume of the syringe reservoir, since the perfusate cannot be easily recirculated in this model.

Perfusate Oxygenation. Mammalian cells require oxygen for aerobic respiration. Oxygen serves as the final electron acceptor in this process, thereby making it essential for normal metabolism in mammalian cells. Dissolved oxygen concentrations in perfusion media must be kept at concentrations of ~200 μM. The perfusion apparatus usually contains an apparatus dedicated to gas exchange, typically referred to as a 'lung'. Perfusion media within the lung may be oxygenated in two principal ways: (i) direct oxygenation (bubbling) and (ii) indirect oxygenation (diffusion through tubing).

Direct Oxygenation (Bubbling). Direct bubbling of oxygen into the perfusate is the easiest method of oxygenating perfusion media. While this method is simple and direct, sterility can be a concern as these are by nature open systems. Foaming is also of particular concern since the presence of bubbles can cause significant problems by disrupting the magnetic field homogeneity within the coil area, affecting the SNR, line shape, and overall quality of the signal. In addition, bubbles may affect the overall viability of the sample, since flow of media will be restricted in that area. One solution is to incorporate degassers into the perfusate flow lines, immediately after the 'lung' (primary removal) or before entry to the NMR sample (secondary, back-up removal). Care must also be taken to allow for sufficient oxygen dissolution in the medium. This can be facilitated by proper adjustment of flow rates and the use of a thermostatically controlled water bath adjusted to physiological temperature.

Indirect Oxygenation (Diffusion through Tubing). Indirect oxygenation requires the use of oxygen-permeable tubing incorporated into the lung vessel enclosure. The medium is run through multiple turns or coils of this permeable tubing while in the lung, facilitating gas exchange of oxygen and CO_2. Advantages to this method are that oxygenation can occur within the closed system. This minimizes exposure of the media to potential contaminants and also simplifies the apparatus. Silicon-rubber tubing is typically used in these applications. In addition to providing sufficient gas permeability this type of tubing has good biocompatibility and can maintain the sterility of the perfusion medium. Examples of tubing with suitable characteristics for indirect gassing include Masterflex® platinum and peroxide-cured silicone tubing (Cole-Palmer).

Owing to the temperature dependence of gas solubility, it is very important that perfusion media temperatures be kept constant throughout the input portion of the perfusion apparatus. Dissolved gases coming out of the solution can again result in bubbles, with deleterious consequences for samples and the acquisition of the MR signal. The temperature of the lung can be easily controlled in this design through the use of a water bath or convection heater enclosing the lung.

Temperature Control

In order to maximize sample viability for perfused MRS, the sample should be kept at the physiological temperature of the host. Warming the perfusion medium and the NMR tube or cell bed best facilitates this. Effective media warming can be accomplished with the use of a water bath with pumping capability. This type of apparatus contains a large water reservoir, digital temperature control and a pump with associated fittings to allow warmed/cooled water to circulate to external areas. Using suitable tubing, water jackets can be constructed to enclose media perfusion lines. Circulation of water through these jackets can keep media lines at as near a constant temperature as possible. Water jackets are more important on the input side of the NMR tube, feeding the sample. Warming the sample in the spectrometer can also be accomplished using the instrument's variable temperature apparatus.

Summary

An overview of the advantages and limitations of perfused MRS of cells and organs has been presented. MRS provides a powerful tool to monitor cellular metabolism in cells and organs, thus allowing us to study the effects of drugs, agonists, and antagonists in controlled environments. Perfused MR of cells and organs is technically demanding, requiring expertise in building and maintaining a perfusion apparatus, and in both cell biology and animal physiology. However, the information content from these experiments is high, and perfused MR remains a valuable tool in translational research from cells to animals to humans and back again.

Acknowledgments

The authors would like to acknowledge the support of the National Institutes of Health, grant number 1-R01 EB018645.

Biographical Sketches

Matthew Milkevitch is an associate professor of Chemistry at Philadelphia University, where he teaches organic and inorganic chemistry. His doctoral training was in Inorganic Chemistry at Virginia Tech. He pursued postdoctoral training on perfused-cell MRS of prostate cancer cells with Jim Delikatny at the University of Pennsylvania before moving to Philadelphia University in 2006. He is director of the Chemistry and Biochemistry programs, and is currently pursuing research on metal-based anticancer agents.

Elizabeth Browning is a research specialist and Technical Director of Optical Imaging in the Radiology Department at the University of Pennsylvania. She completed her PhD in Biomedical Engineering at the University of Virginia in 2009 focusing on mechanobiology in perfused human endothelial cells, evaluating mechano-sensitive biochemical signaling relative to cardiovascular disease. During her postdoctoral fellowship at the University of Pennsylvania she evaluated the role of ischemia-induced reactive oxygen species in vascular remodeling in perfused human and murine endothelial cells, in vivo in a hind limb ischemia model, and in ex vivo isolated perfused mouse lungs using optical imaging.

E. James Delikatny is a professor of Radiology at the University of Pennsylvania and director of the Small Animal Imaging Facility. He obtained his PhD in physical chemistry in solid-state NMR at the University of British Columbia. He did a postdoctoral fellowship at the University of Sydney on MRS of cancer cells, becoming a faculty member in 1996. He moved to the University of Pennsylvania in 2000, where his current research employs multimodal imaging to detect therapy response in cancer cell and animal tumor models. He leads a multidisciplinary research team in the application of MR methodology and the development of optical contrast agents for the study of cellular and small animal models of breast cancer.

Related Articles

In Vivo MRS of Lipids in Adipose Tissue, Bone Marrow, and Liver; Pulse Sequences for Hyperpolarized MRS; Hyperpolarization Methods for MRS; Measuring pHi and pHe by MRS; Cardiac MRS Studies in Rodents and Other Animals; MRS in the Failing Heart: From Mice to Humans; Integration of ^{13}C Isotopomer Methods and Hyperpolarization Provides a Comprehensive Picture of Metabolism; Diffusion-Weighted Magnetic Resonance Spectroscopy; Measuring Biochemical Reaction Rates In Vivo with Magnetization Transfer

References

1. J. D. Glickson, in Encyclopedia of Magnetic Resonance, eds R. K. Harris and R. E. Wasylishen, John Wiley: New York, 1996, Chap. Cells and Cell Systems MRS.
2. A. Mancuso and J. D. Glickson, in Fundamentals of Cell Immobilisation Biotechnology, eds V. Nedovic and R. Willaert, Springer: Dordrecht, 2004, Chap. Applications of NMR Spectroscopy and Imaging to the Study of Immobilised Cell Physiology, 439.
3. H. Degani, S. M. Ronen, and E. Furman-Haran, in NMR in Physiology and Biomedicine, ed. R. J. Gillies, Academic Press, Inc: San Diego, CA, 1994, Chap. Breast cancer: spectroscopy and imaging of cells and tumors, 329.
4. K. A. McGovern, in NMR in Physiology and Biomedicine, ed. R. J. Gillies, Academic Press, Inc: San Diego, CA, 1994, Chap. Bioreactors, 279.
5. P. Lundberg, S. Roy, and P. W. Kuchel, *Immunomethods*, 1994, **4**, 163.
6. B. S. Szwergold, *Annu. Rev. Physiol.*, 1992, **54**, 775.
7. R. T. Eakin, L. O. Morgan, C. T. Gregg, and N. A. Matwiyoff, *FEBS Lett.*, 1972, **28**, 259.
8. R. B. Moon and J. H. Richards, *J. Biol. Chem.*, 1973, **248**, 7276.
9. J. M. Salhany, T. Yamane, R. G. Shulman, and S. Ogawa, *Proc. Natl. Acad. Sci. U. S. A.*, 1975, **72**, 4966.
10. P. B. Garlick, G. K. Radda, and P. J. Seeley, *Biochem. Biophys. Res. Commun.*, 1977, **74**, 1256.
11. J. M. Salhany, S. J. Stohs, L. A. Reinke, G. M. Pieper, and J. M. Hassing, *Biochem. Biophys. Res. Commun.*, 1979, **86**, 1077.
12. P. A. Sehr and G. K. Radda, *Biochem. Biophys. Res. Commun.*, 1977, **77**, 195.
13. S. M. Cohen, R. G. Shulman, and A. C. McLaughlin, *Proc. Natl. Acad. Sci. U. S. A.*, 1979, **76**, 4808.
14. S. M. Cohen and R. G. Shulman, *Philos. Trans. R. Soc. Lond. B Biol. Sci.*, 1980, **289**, 407.
15. I. A. Bailey, D. G. Gadian, P. M. Matthews, G. K. Radda, and P. J. Seeley, *FEBS Lett.*, 1981, **123**, 315.
16. S. M. Cohen, P. Glynn, and R. G. Shulman, *Proc. Natl. Acad. Sci. U. S. A.*, 1981, **78**, 60.
17. A. C. Kuesel, G. Graschew, W. E. Hull, W. Lorenz, and H. W. Thielmann, *NMR Biomed.*, 1990, **3**, 78.
18. E. J. Delikatny, W. A. Cooper, S. Brammah, N. Sathasivam, and D. C. Rideout, *Cancer Res.*, 2002, **62**, 1394.
19. E. J. Delikatny, S. Chawla, D. J. Leung, and H. Poptani, *NMR Biomed.*, 2011, **24**, 592.
20. K. Ugurbil, D. L. Guernsey, T. R. Brown, P. Glynn, N. Tobkes, and I. S. Edelman, *Proc. Natl. Acad. Sci. U. S. A.*, 1981, **78**, 4843.
21. H. Farghali, L. Rossaro, J. S. Gavaler, D. H. Van Thiel, S. R. Dowd, D. S. Williams, and C. Ho, *Biochim. Biophys. Acta*, 1992, **1139**, 105.
22. A. Gasbarrini, A. B. Borle, H. Farghali, C. Bender, A. Francavilla, and D. Van Thiel, *J. Biol. Chem.*, 1992, **267**, 6654.
23. A. Mancuso, A. Zhu, N. J. Beardsley, J. D. Glickson, S. Wehrli, and S. Pickup, *Magn. Reson. Med.*, 2005, **54**, 67.
24. J. C. Chatham, J. R. Forder, J. D. Glickson, and E. M. Chance, *J Biol Chem*, 1995, **270**, 7999.
25. A. D. Sherry, C. R. Malloy, R. E. Roby, A. Rajagopal, and F. M. Jeffrey, *Biochem. J.*, 1988, **254**, 593.
26. O. M. Hyyti, X. H. Ning, N. E. Buroker, M. Ge, and M. A. Portman, *Am. J. Physiol. Endocrinol. Metab.*, 2006, **290**, E372.
27. R. J. DeBerardinis, A. Mancuso, E. Daikhin, I. Nissim, M. Yudkoff, S. Wehrli, and C. B. Thompson, *Proc. Natl. Acad. Sci. U. S. A.*, 2007, **104**, 19345.
28. J. L. Izquierdo-Garcia, P. Viswanath, P. Eriksson, L. Cai, M. Radoul, M. M. Chaumeil, M. Blough, H. A. Luchman, S. Weiss, J. G. Cairncross, J. J. Phillips, R. O. Pieper, and S. M. Ronen, *Cancer Res.*, 2015, **75**, 2999.
29. J. M. O'Donnell, M. J. Fasano, and E. D. Lewandowski, *Magn. Reson. Med.*, 2015, **74**, 330.
30. D. L. Johnston and E. D. Lewandowski, *Circ. Res.*, 1991, **68**, 714.
31. S. M. Cohen, *J. Biol. Chem.*, 1983, **258**, 14294.
32. S. M. Cohen, R. Rognstad, R. G. Shulman, and J. Katz, *J. Biol. Chem.*, 1981, **256**, 3428.
33. S. M. Cohen, *Fed. Proc.*, 1984, **43**, 2657.
34. S. M. Cohen, *Biochemistry*, 1987, **26**, 563.
35. N. Hausler, J. Browning, M. Merritt, C. Storey, A. Milde, F. M. Jeffrey, A. D. Sherry, C. R. Malloy, and S. C. Burgess, *Biochem. J.*, 2006, **394**, 465.
36. C. O. Miller, J. Cao, E. Y. Chekmenev, B. M. Damon, A. D. Cherrington, and J. C. Gore, *Anal. Chem.*, 2015, **87**, 5824.
37. A. A. Shestov, A. Mancuso, S. C. Lee, L. Guo, D. S. Nelson, J. C. Roman, P. G. Henry, D. B. Leeper, I. A. Blair, and J. D. Glickson, *J. Biol. Chem.*, 2016, **291**, 5157.

38. C. S. Ward, H. S. Venkatesh, M. M. Chaumeil, A. H. Brandes, M. Vancriekinge, H. Dafni, S. Sukumar, S. J. Nelson, D. B. Vigneron, J. Kurhanewicz, C. D. James, D. A. Haas-Kogan, and S. M. Ronen, *Cancer Res.*, 2010, **70**, 1296.

39. A. Lodi, S. M. Woods, and S. M. Ronen, *NMR Biomed.*, 2012, **26**, 299.

40. K. R. Keshari, R. Sriram, M. Van Criekinge, D. M. Wilson, Z. J. Wang, D. B. Vigneron, D. M. Peehl, and J. Kurhanewicz, *Prostate*, 2013, **73**, 1171.

41. M. A. Schroeder, H. J. Atherton, D. R. Ball, M. A. Cole, L. C. Heather, J. L. Griffin, K. Clarke, G. K. Radda, and D. J. Tyler, *FASEB J.*, 2009, **23**, 2529.

42. M. E. Merritt, C. Harrison, A. D. Sherry, C. R. Malloy, and S. C. Burgess, *Proc. Natl. Acad. Sci. U. S. A.*, 2011, **108**, 19084.

43. H. Shaghaghi, S. Kadlecek, C. Deshpande, S. Siddiqui, D. Martinez, M. Pourfathi, H. Hamedani, M. Ishii, H. Profka, and R. Rizi, *NMR Biomed.*, 2014, **27**, 939.

44. M. M. Chaumeil, J. M. Lupo, and S. M. Ronen, *Brain Pathol.*, 2015, **25**, 769.

45. M. M. Chaumeil, P. E. Larson, S. M. Woods, L. Cai, P. Eriksson, A. E. Robinson, J. M. Lupo, D. B. Vigneron, S. J. Nelson, R. O. Pieper, J. J. Phillips, and S. M. Ronen, *Cancer Res.*, 2014, **74**, 4247.

46. K. R. Keshari, J. Kurhanewicz, R. Bok, P. E. Larson, D. B. Vigneron, and D. M. Wilson, *Proc. Natl. Acad. Sci. U. S. A.*, 2011, **108**, 18606.

47. P. F. Daly, R. C. Lyon, P. J. Faustino, and J. S. Cohen, *J. Biol. Chem.*, 1987, **262**, 14875.

48. S. E. Franks, A. C. Kuesel, N. W. Lutz, and W. E. Hull, *Anticancer Res*, 1996, **16**, 1365.

49. M. I. Bak and J. S. Ingwall, *Cardiovasc Res*, 2003, **57**, 1004.

50. L. Baillet-Blanco, M. C. Beauvieux, H. Gin, V. Rigalleau, and J. L. Gallis, *Nutr Metab (Lond)*, 2005, **2**, 32.

51. N. Leducq, M. C. Delmas-Beauvieux, I. Bourdel-Marchasson, S. Dufour, J. L. Gallis, P. Canioni, and P. Diolez, *Biochem. J.*, 1998, **336**, 501.

52. J. T. Flaherty, M. L. Weisfeldt, B. H. Bulkley, T. J. Gardner, V. L. Gott, and W. E. Jacobus, *Circulation*, 1982, **65**, 561.

53. J. A. Woods, C. J. Storey, E. E. Babcock, and C. R. Malloy, *J. Cardiovasc. Pharmacol.*, 1998, **31**, 359.

54. J. G. Jones, T. H. Le, C. J. Storey, A. D. Sherry, C. R. Malloy, and K. P. Burton, *Free Radic. Biol. Med.*, 1996, **20**, 515.

55. P. B. Kingsley-Hickman, E. Y. Sako, K. Ugurbil, A. H. From, and J. E. Foker, *J. Biol. Chem.*, 1990, **265**, 1545.

56. M. Milkevitch, H. Shim, U. Pilatus, S. Pickup, J. P. Wehrle, D. Samid, H. Poptani, J. D. Glickson, and E. J. Delikatny, *Biochim. Biophys. Acta*, 2005, **1734**, 1.

57. S. M. Ronen, E. Rushkin, and H. Degani, *Biochim. Biophys. Acta*, 1992, **1138**, 203.

58. P. F. Daly, G. Zugmaier, D. Sandler, M. Carpen, C. E. Myers, and J. S. Cohen, *Cancer Res.*, 1990, **50**, 552.

59. S. M. Ronen, E. Rushkin, and H. Degani, *Biochim. Biophys. Acta*, 1991, **1095**, 5.

60. K. Glunde, E. Ackerstaff, K. Natarajan, D. Artemov, and Z. M. Bhujwalla, *Magn. Reson. Med.*, 2002, **48**, 819.

61. M. Milkevitch, N. J. Beardsley, and E. J. Delikatny, *NMR Biomed.*, 2010, **23**, 473.

62. J. P. Galons, C. Job, and R. J. Gillies, *Magn. Reson. Med.*, 1995, **33**, 422.

63. S. Neubauer, J. B. Newell, and J. S. Ingwall, *Circulation*, 1992, **86**, 302.

64. L. F. Wexler, B. H. Lorell, S. Momomura, E. O. Weinberg, J. S. Ingwall, and C. S. Apstein, *Circ. Res.*, 1988, **62**, 766.

65. R. J. Gillies, Z. Liu, and Z. Bhujwalla, *Am. J. Physiol.*, 1994, **267**, C195.

66. R. G. Spencer, J. A. Balschi, J. S.Leigh Jr, and J. S. Ingwall, *Biophys. J.*, 1988, **54**, 921.

67. E. A. Shoubridge, F. M. Jeffry, J. M. Keogh, G. K. Radda, and A. M. Seymour, *Biochim. Biophys. Acta*, 1985, **847**, 25.

68. I. Constantinidis, I. Rask, R. C. Long Jr, and A. Sambanis, *Biomaterials*, 1999, **20**, 2019.

69. R. J. Gillies, J. P. Galons, K. A. McGovern, P. G. Scherer, Y. H. Lien, C. Job, R. Ratcliff, F. Chapa, S. Cerdan, and B. E. Dale, *NMR Biomed.*, 1993, **6**, 95.

70. T. L. Richards, F. Terrier, R. E. Sievers, M. J. Lipton, M. E. Moseley, and C. B. Higgins, *Invest. Radiol.*, 1987, **22**, 638.

71. K. Ugurbil, M. Petein, R. Maidan, S. Michurski, J. N. Cohn, and A. H. From, *FEBS Lett.*, 1984, **167**, 73.

72. C. Liess, G. K. Radda, and K. Clarke, *Magn. Reson. Med.*, 2000, **44**, 208.

73. P. C. van Zijl, C. K. Jones, J. Ren, C. R. Malloy, and A. D. Sherry, *Proc. Natl. Acad. Sci. U. S. A.*, 2007, **104**, 4359.

74. P. C. Van Zijl, C. T. Moonen, P. Faustino, J. Pekar, O. Kaplan, and J. S. Cohen, *Proc. Natl. Acad. Sci. U. S. A.*, 1991, **88**, 3228.

75. M. Bental and C. Deutsch, *Immunomethods*, 1994, **4**, 148.

76. H. Kusuoka, M. Kitakaze, Y. Koretsune, M. Inoue, and E. Marban, *Jpn. Circ. J.*, 1991, **55**, 878.

77. S. Cabanac, M. C. Malet-Martino, M. Bon, R. Martino, J. F. Nedelec, and J. L. Dimicoli, *NMR Biomed.*, 1988, **1**, 113.

78. N. Bansal, M. J. Germann, V. Seshan, G. T.Shires III, C. R. Malloy, and A. D. Sherry, *Biochemistry*, 1993, **32**, 5638.

79. S. K. Miller, W. J. Chu, G. M. Pohost, and G. A. Elgavish, *Magn. Reson. Med.*, 1991, **20**, 184.

80. J. S. Tauskela, J. M. Dizon, J. Whang, and J. Katz, *J. Magn. Reson.*, 1997, **127**, 115.

81. J. M. Colet, N. Bansal, C. R. Malloy, and A. D. Sherry, *Magn. Reson. Med.*, 1999, **41**, 1127.

82. V. D. Schepkin, I. O. Choy, T. F. Budinger, D. Y. Obayashi, S. E. Taylor, W. M. DeCampli, S. C. Amartur, and J. N. Young, *Magn. Reson. Med.*, 1998, **39**, 557.

83. E. N. Aguor, C. W. van de Kolk, F. Arslan, M. G. Nederhoff, P. A. Doevendans, G. Pasterkamp, G. J. Strijkers, and C. J. van Echteld, *Int. J. Cardiovasc. Imaging*, 2013, **29**, 343.

84. P. Lundberg, S. J. Berners-Price, S. Roy, and P. W. Kuchel, *Magn. Reson. Med.*, 1992, **25**, 273.

85. R. H. Knop, C. W. Chen, J. B. Mitchell, A. Russo, S. McPherson, and J. S. Cohen, *Biochim. Biophys. Acta*, 1984, **804**, 275.

86. P. F. Daly, R. C. Lyon, E. J. Straka, and J. S. Cohen, *FASEB J.*, 1988, **2**, 2596.

87. U. Pilatus, E. Ackerstaff, D. Artemov, N. Mori, R. J. Gillies, and Z. M. Bhujwalla, *Neoplasia*, 2000, **2**, 273.

88. R. Benelli, G. Frumento, A. Albini, and D. M. Noona, Models of Inflammatory Processes in Cancer, Birkhauser Verlag: Berlin, 2006.

89. K. S. Narayan, E. A. Moress, J. C. Chatham, and P. B. Barker, *NMR Biomed.*, 1990, **3**, 23.

90. U. Pilatus, H. Shim, D. Artemov, D. Davis, P. C. van Zijl, and J. D. Glickson, *Magn. Reson. Med.*, 1997, **37**, 825.

91. U. Sonnewald, S. B. Petersen, J. Krane, N. Westergaard, and A. Schousboe, *Magn. Reson. Med.*, 1992, **23**, 166.

92. M. Neeman, E. Rushkin, A. Kadouri, and H. Degani, *Magn. Reson. Med.*, 1988, **7**, 236.

93. P. M. Alves, U. Flogel, A. Brand, D. Leibfritz, M. J. Carrondo, H. Santos, and U. Sonnewald, *Dev. Neurosci.*, 1996, **18**, 478.

94. A. Mancuso, N. J. Beardsley, S. Wehrli, S. Pickup, F. M. Matschinsky, and J. D. Glickson, *Biotechnol. Bioeng.*, 2004, **87**, 835.

95. R. J. Gillies, P. G. Scherer, N. Raghunand, L. S. Okerlund, R. Martinez-Zaguilan, L. Hesterberg, and B. E. Dale, *Magn. Reson. Med.*, 1991, **18**, 181.

96. K. R. Keshari, J. Kurhanewicz, R. E. Jeffries, D. M. Wilson, B. J. Dewar, M. Van Criekinge, M. Zierhut, D. B. Vigneron, and J. M. Macdonald, *Magn. Reson. Med.*, 2010, **63**, 322.

97. Y. Martin and P. Vermette, *Biomaterials*, 2005, **26**, 7481.

98. V. Olejnickova, M. Novakova, and I. Provaznik, *Med. Biol. Eng. Comput.*, 2015, **53**, 669.

99. R. M. Bell, M. M. Mocanu, and D. M. Yellon, *J. Mol. Cell. Cardiol.*, 2011, **50**, 940.

100. M. Skrzypiec-Spring, B. Grotthus, A. Szelag, and R. Schulz, *J. Pharmacol. Toxicol. Methods*, 2007, **55**, 113.

101. G. J. Gores, L. J. Kost, and N. F. LaRusso, *Hepatology*, 1986, **6**, 511.

102. J. H. Exton, *Methods Enzymol.*, 1975, **39**, 25.